

See discussions, stats, and author profiles for this publication at: <https://www.researchgate.net/publication/251233687>

Surface Passivation of Gallium Nitride by Ultrathin RF-Magnetron Sputtered Al₂O₃ Gate

ARTICLE in ACS APPLIED MATERIALS & INTERFACES · JULY 2013

Impact Factor: 6.72 · DOI: 10.1021/am402333t · Source: PubMed

CITATIONS

5

READS

28

2 AUTHORS:



[Hock Jin Quah](#)

Universiti Sains Malaysia

38 PUBLICATIONS 193 CITATIONS

[SEE PROFILE](#)



[K.Y. Cheong](#)

Universiti Sains Malaysia

207 PUBLICATIONS 1,689 CITATIONS

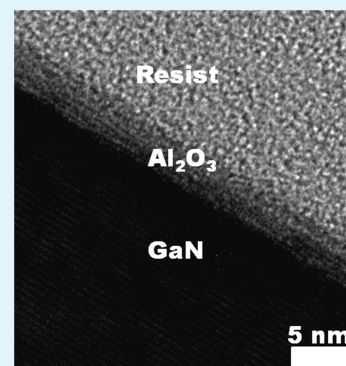
[SEE PROFILE](#)

Surface Passivation of Gallium Nitride by Ultrathin RF-Magnetron Sputtered Al₂O₃ Gate

Hock Jin Quah and Kuan Yew Cheong*

Electronic Materials Research Group, School of Materials & Mineral Resources Engineering, Engineering Campus, Universiti Sains Malaysia, 14300 Nibong Tebal, Seberang Perai Selatan, Penang, Malaysia

ABSTRACT: An ultrathin RF-magnetron sputtered Al₂O₃ gate on GaN subjected to postdeposition annealing at 800 °C in O₂ ambient was systematically investigated. A cross-sectional energy-filtered transmission electron microscopy revealed formation of crystalline Al₂O₃ gate, which was supported by X-ray diffraction analysis. Various current conduction mechanisms contributing to leakage current of the investigated sample were discussed and correlated with metal-oxide-semiconductor characteristics of this sample.



KEYWORDS: gallium nitride, aluminum oxide, conduction mechanisms, passivation, oxygen

INTRODUCTION

A dramatic upsurge in demand of energy consumption throughout the world has hastened the momentum in developing next-generation metal-oxide-semiconductor (MOS) devices for high-power and high-temperature applications using gallium nitride (GaN) as the semiconductor substrate. GaN is ideally suited for these applications because of its wide bandgap (3.4 eV), large critical electric field (3 MV/cm), high electron mobility, as well as good thermal conductivity and stability.^{1,2} To produce an energy-efficient GaN-based MOS device, a high-quality gate oxide is of prior concern to achieve low leakage current and high transverse electric field of the devices.² Relatively low dielectric constant (k) and high- k gate oxides have been extensively investigated on the GaN.^{1,2} The relatively low- k gate oxides, such as SiN_xO_y ($k = 5.0$ – 7.5) or SiO₂ ($k = 3.9$)² with low dielectric breakdown field (E) may not assist in fabricating energy efficient GaN-based MOS devices. Breakdown of the devices is constrained by shortcomings of SiN_xO_y or SiO₂ gate rather than exploiting high E possessed by the GaN substrate. This inadequacy can be prevailed using high- k gate oxides in the GaN-based MOS devices.

Particular interest has developed toward utilizing aluminum oxide (Al₂O₃; $k = 8$ – 10) as a high- k gate in the GaN-based MOS devices in recent times.^{3,4} This is owing to the presence of the Al₂O₃ gate in amorphous phase regardless of deposition techniques and ambient.^{3–6} The amorphous phase was preserved after postdeposition annealing (PDA) at 800 °C.^{4,5} The lowest interface trap density, the smallest hysteresis, and the lowest leakage current density (J) were attained by the amorphous Al₂O₃ formed at 800 °C.^{4,5} However, Toyoda et al. reported transformation of the amorphous phase to crystalline

phase at this temperature (800 °C).⁶ The crystalline Al₂O₃ formed at 800 °C has demonstrated larger band gap ($E_g = 8.3$ eV) and conduction band offset with respect to GaN ($\Delta E_c = 3.5$ eV) when compared with the amorphous Al₂O₃ ($E_g = 7.6$ eV and $\Delta E_c = 2.7$ eV).⁶ Acquisition of larger E_g and ΔE_c for the crystalline Al₂O₃ is anticipated to provide better electrical performance since conduction of charges through the conduction band of the oxide would be impeded though literatures^{4,5} reported that the J was deteriorated at PDA beyond 800 °C due to presence of the crystalline Al₂O₃. In this work, crystalline Al₂O₃ was formed on GaN substrate during PDA at 800 °C in oxygen (O₂) ambient. A better J – E characteristic of the crystalline Al₂O₃ is shown in Figure 1 in comparison with replotted J – E characteristics of formerly reported Al₂O₃/GaN^{3,7–12} structure using linear approximation method. Besides, the obtained J – E characteristic in this work has surpassed the J – E characteristics demonstrated by majority reported gate oxide materials.² A detailed analysis on the structural and electrical performance of Al₂O₃/GaN structure that contributed to this observation has been provided in this letter.

EXPERIMENTAL SECTION

Commercially purchased Si-doped (n-type) GaN epitaxial layer [$7\ \mu\text{m}$ thick and doping concentration of $(1\text{--}9) \times 10^{18}\ \text{cm}^{-3}$] grown on sapphire substrate was RCA cleaned prior to deposition of Al₂O₃ film ($\sim 6\ \text{nm}$) using RF-magnetron sputtering system (HHV Auto500). Deposition parameters reported in previous work² at a power of 160

Received: June 16, 2013

Accepted: July 22, 2013

Published: July 22, 2013



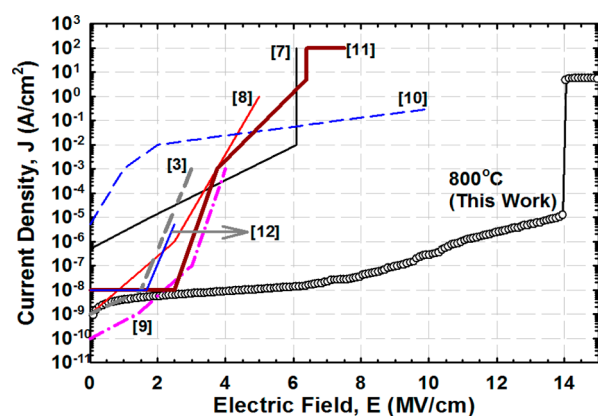


Figure 1. Comparison of J - E characteristics of reported $\text{Al}_2\text{O}_3/\text{GaN}$ system.

We were used during deposition of the Al_2O_3 film. PDA at 800 °C (heating and cooling rate = 10 °C/min) in O_2 ambient for 30 min was performed in horizontal tube furnace. The Al_2O_3 layer was selectively etched by $\text{HF}:\text{H}_2\text{O}$ solution and Al was evaporated on top of the oxide using thermal evaporator (AUTO 306). Subsequently, an array of $2.5 \times 10^{-3} \text{ cm}^2$ Al gate electrode was defined using photolithography process. Figure 2 shows a schematic illustration of the fabricated Al/

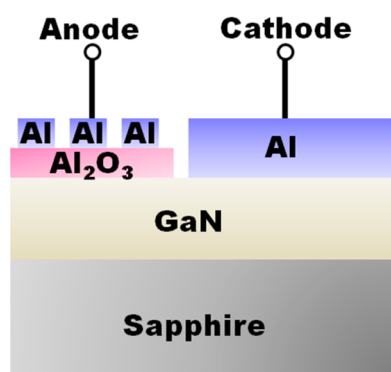


Figure 2. Schematic illustration of Al/ Al_2O_3 /GaN-based MOS structure.

$\text{Al}_2\text{O}_3/\text{GaN}$ -based MOS structure. Physical characteristics of the oxide were analyzed using energy-filtered transmission electron microscopy (EFTEM; Zeiss LIBRA 200) and X-ray diffraction (XRD; P8 Advan-Bruker). Gate thickness and refractive index were estimated at 5 different locations using MProbe thin film measurement system (Semiconsoft UVVisSR) at a wavelength of 632.8 nm. High frequency (HF; 100 kHz) capacitance-voltage (C - V) and current-voltage (I - V) characteristics of the MOS test structures were measured by Keithley 4200-SCS and Agilent 4156C, respectively.

RESULTS AND DISCUSSION

EFTEM image of RF-magnetron sputtered Al_2O_3 gate on GaN, which has been subjected to PDA at 800 °C is shown in inset of Figure 3. Detection of fringes in region of Al_2O_3 gate revealed the formation of crystalline structure, which was supported from XRD with the detection of Al_2O_3 phase (ICDD file no. 01-074-0323) oriented in (110) and (024) planes (not shown). Besides, EFTEM also disclosed the absence of interfacial layer (IL) in the $\text{Al}_2\text{O}_3/\text{GaN}$ system. XRD supported this claim since no $\beta\text{-Ga}_2\text{O}_3$ phase was detected, wherein crystalline $\beta\text{-Ga}_2\text{O}_3$ phase is formed at 800 °C.² The absence of IL in this work is in agreement with the reported atomic-layer-deposited (ALD) Al_2O_3 on GaN PDA at 800 °C.³ Average

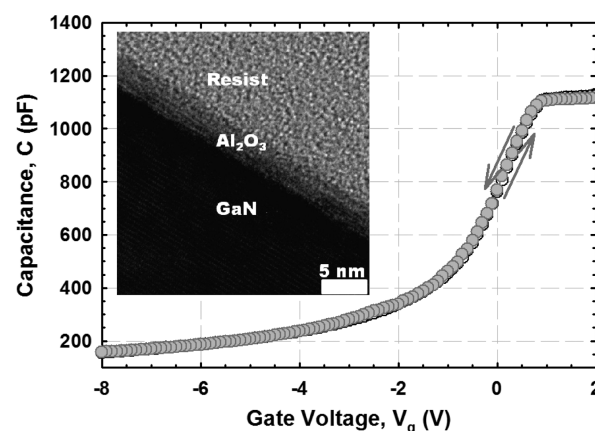


Figure 3. C - V curve of Al/ Al_2O_3 /GaN-based MOS structure. Inset shows cross-sectional EFTEM image of $\text{Al}_2\text{O}_3/\text{GaN}$ system.

measured thickness of the Al_2O_3 gate at 20 different locations from the EFTEM (3.6 nm) is comparable with that acquired from MProbe (~ 4.4 nm).

Figure 3 presents the HF C - V measurement of this sample, which is swept bidirectionally from -8 to $+2$ V. Deep depletion is observed in negative bias because of the slow generation rate of minority carriers at room temperature by the GaN. A negative flatband voltage shift (ΔV_{FB}) is perceived, indicating existence of positively charged traps in the oxide. This is shown via acquisition of a positive effective oxide charge, Q_{eff} of $2.1 \times 10^{12} \text{ cm}^{-2}$ in the oxide, which is comparable with reported values of ALD Al_2O_3 (1.2 – $1.3 \times 10^{12} \text{ cm}^{-2}$) on GaN.^{4,13} A minute hysteresis in the C - V curves (Figure 3) indicates existence of slow trap with density of $1.1 \times 10^{11} \text{ cm}^{-2}$ in this oxide. Presence of donor traps in the oxide may contribute to this, whereby tendency to capture and release injected electrons from the traps in the oxide is low. Terman's method¹⁴ was used to extract interface trap density ($D_{\text{it}} = 1.1 \times 10^{13} \text{ cm}^{-2} \text{ eV}^{-1}$ at $E_{\text{c}} - E_{\text{t}} = 0.50 \text{ eV}$), which is comparable with density reported by ALD Al_2O_3 ($\sim 1.0 \times 10^{13} \text{ cm}^{-2} \text{ eV}^{-1}$)³ at similar $E_{\text{c}} - E_{\text{t}}$.

Figure 4 shows J - E characteristics of this sample measured at 25–175 °C. Current conduction behavior for this sample adheres to Lampert's theory of space-charge-limited conduction (SCLC) at low V_{g} , which is bounded by 3 regions known as Ohm's law ($J_{\text{ohm}} = qn_0\mu(V_{\text{g}}/d)$), SCLC that follows Mott-Gurney law ($J_{\text{Mott-Gurney}} = 9\epsilon_r\epsilon_0\mu V_{\text{g}}^2/8d^3$), and trap-filled-limit

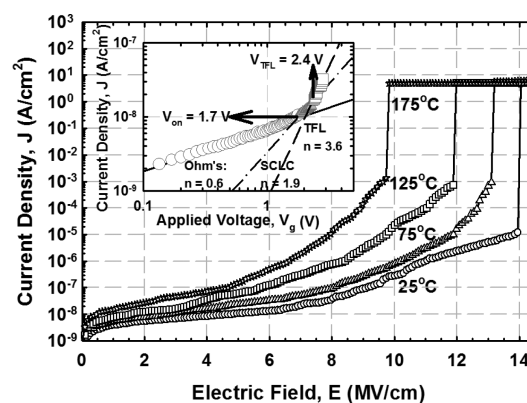


Figure 4. J - E characteristic of $\text{Al}_2\text{O}_3/\text{GaN}$ MOS capacitor measured from 25 to 175 °C. Inset shows a typical space-charge-limited conduction plot of this sample measured at 25 °C.

conduction (TFL; $J_{\text{TFL}} = B(V_g^n/d^{2l+1})$); where q , n_o , μ , V_g , d , ϵ_p , ϵ_o , B and l are electronic charge, free charge carriers concentration in thermal equilibrium, charge carrier mobility in Al_2O_3 , gate voltage, Al_2O_3 gate thickness, dynamic dielectric constant, permittivity of free space, a constant, and a constant related to trap distribution and temperature, respectively.¹⁵ Acquisition of a gradient (0.6–0.7) extracted from the $\log(J) - \log(V_g)$ (inset of Figure 4) at low V_g indicates occurrence of Ohmic conduction, which is comparable to 1. When the V_g approaches V_{on} , carrier transit time ($\tau_c = d^2/\mu V_{\text{on}}$) is equal to dielectric relaxation time ($\tau_d = \epsilon_r \epsilon_o / q n \mu$).¹⁵ At $V_g \geq V_{\text{on}}$, SCLC is dominating the current conduction as the extracted gradient (1.8–2.4) is close to 2. Because V_{on} (0.8–1.7 V) and τ_c $[(1.2 - 1.3) \times 10^{-2} \text{ s}]$ are identified, μ $[(0.6 - 1.4) \times 10^{-11} \text{ cm}^2 \text{ V}^{-1} \text{ s}^{-1}]$ in Al_2O_3 gate is determined. Further increase in the V_g to TFL voltage ($V_{\text{TFL}} = q N_t d^2 / 2 \epsilon_r \epsilon_o$) leads to a shift from SCLC to TFL conduction and the extracted gradient from TFL region is 3.5–6.2. A reduction in V_{TFL} from 2.4 to 1.7 V with respect to measurement temperature suggests that higher temperature has triggered thermally generated carriers to occupy the available traps in the oxide. Density of traps (N_t) present in the oxide is $(4.5 - 6.5) \times 10^{19} \text{ cm}^{-3}$. A reduction in the N_t with the increase in measurement temperature has enhanced number of free moving carriers in the oxide, which is related to the increment in μ . The attainment of a higher μ and N_t have resulted in an increase in J at higher measurement temperature.

Beyond TFL region, Schottky Emission (SE), Poole–Frenkel (PF) emission, and Fowler–Nordheim (FN) tunneling could be the governing conduction mechanisms. Datafit version 9.0.59 was used to perform a nonlinear curve fitting on the acquired J – E results with these conduction mechanisms. SE is termed as thermionic emission of electrons over the oxide–GaN surface barrier.¹⁶ Obtained experimental J – E results that are fitted well with SE are shown in Figure 5. SE is deemed to be the dominating

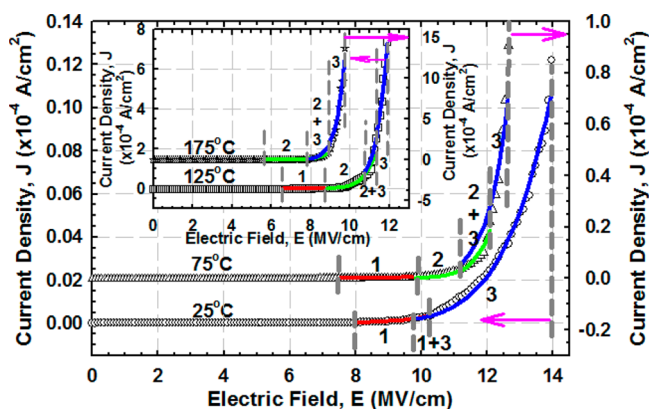


Figure 5. Experimental data (symbol) for sample measured at 25–75 °C and 125–175 °C (inset) fitted well with SE (red line), PF emission (green line), and FN tunneling (blue line) models. The numbering 1–3 represents dominance of SE, PF emission, and FN tunneling, respectively.

conduction when the extracted ϵ_r value is comparable with optical dielectric constant (ϵ_{opt}) of the film, $[\epsilon_r^{1/2} = \epsilon_{\text{opt}}^{1/2} = n]$, where n is the refractive index of the film ($n = 1.69 - 1.78$) and the nonlinear curve fitting yields a coefficient of determination, r^2 of higher than 0.75. The J of this sample is governed by SE at measurement temperature from 25 to 125 °C (Figure 5) and the extracted $\epsilon_r^{1/2}$ is 1.92–2.22. An increment in barrier height ($\Phi_B = 1.052 - 1.224 \text{ eV}$) as a function of measurement

temperature denotes triggering of electron emission to overcome a higher surface barrier with the enhancement of measurement temperature, which leads to stimulation of J .

When E is further enhanced, PF emission is governing the J and region fitted well with PF emission model is shown in Figure 5. Trap energy level ($\Phi_t = 1.506 - 1.584 \text{ eV}$) is obtained for sample measured from 75 to 175 °C as the attained $\epsilon_r^{1/2}$ (1.63–1.90) value is comparable with n . An increment in the measurement temperature has contributed to a rise in the Φ_t , whereby the carriers trapped by the traps that are located deeper in the oxide is released. The positive Q_{eff} present in the oxide is postulated to cause PF emission to occur. Initially, the positive Q_{eff} will capture the injected electrons to form neutral traps. Tendency of detrapping the charges from the positive Q_{eff} through PF emission is low. Hence, a higher E and measurement temperature is required for this process to happen than SE.

FN tunneling, which is a tunneling process that allows injected charged carriers to pass through triangular energy barrier into conduction band of the Al_2O_3 gate¹⁶ has been used to determine Φ_B between the Al_2O_3 gate and GaN, in which the Φ_B is referred to as the conduction band offset (ΔE_c) between the Al_2O_3 gate and GaN. Figure 5 shows regions fitted well with the model. The Φ_B value estimated from FN tunneling is 2.97–4.81 eV at 25–175 °C, which is higher than that obtained from SE. The attainment of a higher Φ_B from FN tunneling is due to the occurrence of this mechanism at a higher E , wherein the slope of energy band in the Al_2O_3 gate and GaN becomes steeper. The obtained Φ_B (2.97 eV) at 25 °C in this work is larger than the reported Φ_B for ALD Al_2O_3 (2.20 eV)³ and metal–organic decomposed CeO_2 (1.13 eV) spin-coated¹⁷ on GaN. Unfortunately, the obtained Φ_B (2.97 eV) from FN tunneling model in this work is lower than the computed ΔE_c of chemical vapor deposited Al_2O_3 on GaN (3.50 eV)⁶ subjected to similar PDA temperature using X-ray absorption spectroscopy (XAS). A discrepancy of 0.53 eV between the acquired ΔE_c may be related to the usage of extraction methods. This could be supported based on previous investigations, wherein a difference of 0.50 eV has been determined between the ΔE_c attained using FN tunneling model for the as-deposited Al_2O_3 gate using ALD on GaN (2.20 eV)³ and the ΔE_c acquired using XAS for the as-deposited Al_2O_3 gate using CVD on GaN (2.70 eV).⁶ When XAS and ultraviolet photoelectron spectroscopy (UPS) characterizations are utilized to compute the ΔE_c for CVD (2.80 eV)⁶ and ALD (3.00 eV)¹⁸ Al_2O_3 gate on GaN substrate, respectively, subjected to postdeposition annealing (PDA) at 700 °C, the acquired ΔE_c values did not differ appreciably. This indicates that extraction of ΔE_c value using FN tunneling model may differ considerably with a limit of approximately 0.5 eV from XAS/UPS characterization. Thus, it is believed that the quality of RF-magnetron sputtered Al_2O_3 gate on GaN substrate in this work is comparable with CVD Al_2O_3 gate on GaN substrate⁶ yet better than ALD Al_2O_3 gate on GaN.³ A combination of SE and FN tunneling as well as PF emission and FN tunneling mechanisms governing the J of investigated sample at 25 °C and 75–175 °C, respectively, has been also shown in Figure 5.

Based on the aforementioned discussion, the Al_2O_3 gate, which has been RF-magnetron sputtered on GaN substrate could serve as a good passivation layer. This is supported through the acquisition of a higher Φ_B using FN tunneling model for the RF-magnetron sputtered Al_2O_3 gate (2.97 eV)

than ALD Al_2O_3 gate (2.20 eV) on GaN substrate³ and the acquisition of a better J – E characteristics as shown in Figure 1. It has been reported that the presence of dangling bonds on the surface of GaN substrate will act as electrically active defects.^{19,20} These active defects will form defect states within the band gap of the GaN substrate that leads to high leakage current. Initially, these defect states will capture the injected electrons from valence band of the substrate and act as scattering centers. These scattering centers will stimulate injection of electrons to overcome the conduction band of the substrate. Therefore, the presence of electrically active defects on the surface of GaN substrate needs to be passivated by Al_2O_3 gate to become passive defects and improved the J – E characteristic. Besides, the good interface quality of RF-magnetron sputtered Al_2O_3 gate on GaN substrate ($D_{\text{it}} = 1.1 \times 10^{13} \text{ cm}^{-2} \text{ eV}^{-1}$ at $E_{\text{c}} - E_{\text{t}} = 0.50 \text{ eV}$), which is comparable with the atomic layer deposited (ALD) Al_2O_3 gate on GaN substrate ($D_{\text{it}} = 1.0 \times 10^{13} \text{ cm}^{-2} \text{ eV}^{-1}$ at $E_{\text{c}} - E_{\text{t}} = 0.50 \text{ eV}$)³ further supports that the Al_2O_3 gate has passivated the surface of GaN substrate. Moreover, a good oxide quality is of importance to determine good passivation behavior of the Al_2O_3 . This has been demonstrated through the acquisition of positive Q_{eff} in the Al_2O_3 that has assisted in enhancing the J – E characteristic. The presence of positive Q_{eff} would assist in capturing the injected electrons to form neutral traps instead of breaking the network of Al_2O_3 . Hence, a higher E is needed to break the network of Al_2O_3 as well as to detrapp charges from the neutral traps via PF emission.

CONCLUSION

In conclusion, an ultrathin polycrystalline Al_2O_3 gate deposited on GaN substrate was successfully formed at 800 °C in O_2 ambient. MOS characteristics of Al/ Al_2O_3 /GaN were reported in this work. Various possible current conduction mechanisms contributing to the leakage current of this sample were identified. These current conduction mechanisms were dependent on measurement temperature.

AUTHOR INFORMATION

Corresponding Author

*E-mail: cheong@eng.usm.my. Tel: +604-599 5259. Fax: +604-594 1011.

Notes

The authors declare no competing financial interest.

ACKNOWLEDGMENTS

H.J.Q. acknowledges financial support given by Universiti Sains Malaysia, The USM RU-PRGS (8044041), and The Universiti Sains Malaysia Vice Chancellor's Award.

REFERENCES

- (1) Chang, S. J.; Wang, C. K.; Su, Y. K.; Chang, C. S.; Lin, T. K.; Ko, T. K.; Liu, H. L. *J. Electrochem. Soc.* **2005**, *152*, G423–G426.
- (2) Quah, H. J.; Cheong, K. Y. *IEEE Trans. Electron Devices* **2012**, *59*, 3009–3016.
- (3) Hori, Y.; Mizue, C.; Hashizume, T. *Jpn. J. Appl. Phys.* **2010**, *49*, 080201–1–080201–3.
- (4) Ostermaier, C.; Lee, H. C.; Hyun, S. Y.; Ahn, S. I.; Kim, K. W.; Cho, H. I.; Ha, J. B.; Lee, J. H. *Phys. Stat. Sol. (c)* **2008**, *5*, 1992–1994.
- (5) Wu, Y. Q.; Shen, T.; Ye, P. D.; Wilk, G. D. *Appl. Phys. Lett.* **2007**, *90*, 143504–1–143504–3.
- (6) Toyoda, S.; Shinohara, T.; Kumigashira, H.; Oshima, M.; Kato, Y. *Appl. Phys. Lett.* **2012**, *101*, 231607–1–231607–4.

- (7) Cico, K.; Kuzmik, J.; Gregusova, D.; Stoklas, R.; Lalinsky, T.; Georgakilas, A.; Pogany, D.; Frohlich, K. *Microelectron. Reliab.* **2007**, *47*, 790–793.
- (8) Chang, Y. H.; Chiu, H. C.; Chang, W. H.; Kwo, J.; Tsai, C. C.; Hong, J. M.; Hong, M. *J. Cryst. Growth* **2009**, *311*, 2084–2086.
- (9) Chang, Y. C.; Huang, M. L.; Chang, Y. H.; Lee, Y. J.; Chiu, H. C.; Kwo, J.; Hong, M. *Microelectron. Eng.* **2011**, *88*, 1207–1210.
- (10) Basu, S.; Singh, P. K.; Huang, J. J.; Wang, Y. H. *J. Electrochem. Soc.* **2007**, *154*, H1041–H1046.
- (11) Lecce, V. D.; Krishnamoorthy, S.; Esposto, M.; Hung, T. H.; Chini, A.; Rajan, S. *Electron. Lett.* **2012**, *48*, 1–2.
- (12) Hung, T. H.; Krishnamoorthy, S.; Esposto, M.; Nath, D. N.; Park, P. S.; Rajan, S. *Appl. Phys. Lett.* **2013**, *102*, 072105–1–072105–4.
- (13) Nepal, N.; Garces, N. Y.; Meyer, D. J.; Hite, J. K.; Mastro, M. A.; C. R. E., Jr. *Appl. Phys. Exp.* **2011**, *4*, 055802–1–055802–3.
- (14) Schroder, D. K. *Semiconductor Material and Device Characterization*; Wiley: New York, 1998; p 337.
- (15) Quah, H. J.; Cheong, K. Y. *Sci. Adv. Mater.* **2013**, DOI: 10.1166/sam.2013.1647.
- (16) Cheong, K. Y.; Moon, J. H.; Kim, H. J.; Bahng, W.; Kim, N. K. *J. Appl. Phys.* **2008**, *103*, 084113–1–084113–8.
- (17) Quah, H. J.; Cheong, K. Y.; Hassan, Z.; Lockman, Z. *Electrochem. Solid-State Lett.* **2010**, *13*, H116–H118.
- (18) Coan, M. R.; Woo, J. H.; Johnson, D.; Gatabi, I. R.; Harris, H. R. *J. Appl. Phys.* **2012**, *112*, 024508–1–024508–6.
- (19) Moustakas, T. D. In *Gallium Nitride (GaN) II: Semiconductors and Semimetals*; Pankove, J. I., Moustakas, T. D., Eds.; Academic Press: San Diego, 1999; Vol. 57, p 73.
- (20) Lenahan, P. M. In *Defects in Microelectronic Materials and Devices*; Fleetwood, D. M., Pantelides, S. T., Schrimpf, R. D., Eds.; CRC Press: Boca Raton, FL, 2009; p 164.